□□□ □□ □ □
□ □ □ □
□ □□ □ □
□
□□□

□

□

□

Theorem 2.5 (Minimizing geodesics, [**8**, **9**]). *Let $a_0, a_2 > 0$ and $a_1 \geq 0$. Then, given two curves c_0, c_1 in the same connected component of $\mathrm{Imm}(S^1, \mathbb{R}^d)$, there exists a minimizing geodesic connecting them. Furthermore, there exists a minimizing geodesic connecting the shapes $\pi(c_0)$ and $\pi(c_1)$ in $\mathcal{S}(S^1, \mathbb{R}^d)$.*

Remark 2.6 (Elastic metrics). Closely related to the Sobolev metrics described here is the family of elastic metrics [**21**], which in the planar case is given by

$$G_c(h,k) = \int_{S^1} a^2 \langle D_s h, n \rangle \langle D_s k, n \rangle + b^2 \langle D_s h, v \rangle \langle D_s k, v \rangle ds.$$

Here a, b are constants and v, n denote the unit tangent and normal vectors to c. Two special cases deserve to be highlighted: for $a = 1$, $b = \frac{1}{2}$ [**27**] and $a = b$ [**55**] there exist nonlinear transforms, the square root velocity transform and the basic mapping, that greatly simplify the numerical computation of geodesics. Both of these metrics have been applied to a variety of problems in shape analysis. We note that the elastic metric with $a = b$ corresponds to a first order Sobolev metric as in Def. 2.1 with $a_0 = a_2 = 0$ and $a_1 = a^2 = b^2$. As it has no L^2-part, it is a Riemannian metric only on the space of curves modulo translations.

3 Numerical implementation

3.1 Discretization

We discretize curves using B-splines; $c = \sum_{j=1}^{N_\theta} d_j C_j(\theta)$, where C_j are the B-splines of degree n_θ, defined on a uniform periodic knot sequence, with all knots of multiplicity one. Observe that $C_j \in C^{n_\theta - 1}([0, 2\pi])$. A path of curves can then be represented using tensor product B-splines, i.e.,

$$c(t, \theta) = \sum_{i=1}^{N_t} \sum_{j=1}^{N_\theta} d_{i,j} B_i(t) C_j(\theta). \tag{1}$$

Here B_i are the B-splines defined on the interval $[0, 1]$, with uniform knots and full multiplicity at the end points, $B_i \in C^{n_t - 1}([0, 1])$. This implies that the boundary curves are given by $c(0, \theta) = \sum_{j=1}^{N_\theta} d_{1,j} C_j(\theta)$ and $c(1, \theta) = \sum_{j=1}^{N_\theta} d_{N_t,j} C_j(\theta)$.

Under the identification of S^1 with $\mathbb{R}/[0, 2\pi]$, diffeomorphisms $\psi: S^1 \to S^1$ can be written as $\psi = \mathrm{id} + \phi$, where ϕ is a periodic function. We choose to discretize $\phi(\theta) = \sum_{i=1}^{N_\phi} \phi_i D_i(\theta)$, where D_i are B-splines of degree n_ϕ, defined on a uniform periodic knot sequence, similarly to C_j. The identity can be written in a B-spline basis using the *Greville abscissas* ξ_i, i.e., $\mathrm{id} = \sum_{i=1}^{N_\phi} \xi_i D_i$. Due to the positivity of B-splines, the condition $\psi' > 0$ ensuring that ψ is a diffeomorphism takes the form

$$\phi_{i-1} - \phi_i < \xi_i - \xi_{i-1}. \tag{2}$$

To speed up convergence, we introduce an additional variable $\alpha \in \mathbb{R}$ representing constant shifts of the reparametrization. The resulting redundancy is eliminated by the constraint

$$\sum_{i=1}^{N_\phi} \phi_i = 0. \tag{3}$$

To compute the energy of paths (1), we use Gaussian quadrature on each interval between subsequent knots. Evaluating paths (and their derivatives) at the quadrature points is a simple multiplication of the spline collocation matrix with the vector of control points.
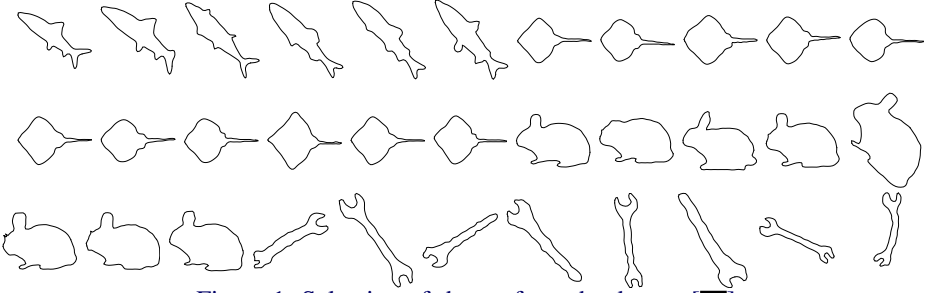
Figure 1: Selection of shapes from the dataset [14].

3.2 Geodesics and Karcher means

From now on we work with plane curves ($d = 2$). The boundary value problem for geodesics consists of minimizing the discretized energy (2) over all paths $c:[0,1] \times [0,2\pi] \to \mathbb{R}^2$, mappings $\psi = \mathrm{id} + \phi : S^1 \to S^1$, shifts of the reparametrization $\alpha \in \mathbb{R}$, and rotations R_β around the origin by an angle $\beta \in [0,2\pi)$, subject to the constraints (2), (3), and

$$c(0,\cdot) = c_0(\cdot), \qquad c(1,\cdot) = R_\beta(c_1(\psi(\cdot) - \alpha) + v),$$

where $c_0, c_1 : [0,2\pi] \to \mathbb{R}^2$ are given boundary curves. This is a finite dimensional constrained optimization problem, which we solve using Matlab's interior point method `fmincon`. We achieved major performance improvements by fine-tuning the implementations of the gradient and hessian of the energy functional.

In the initial value problem for geodesics, the initial value and initial velocity of the sought geodesic are given. As described in Sect. 2, geodesics on $\mathcal{S}(S^1, \mathbb{R}^d)$ can be lifted to horizontal geodesics on $\mathrm{Imm}(S^1, \mathbb{R}^d)$. Thus, solving the geodesic initial value problem for unparametrized curves reduces to solving the problem for parametrized curves with horizontal initial velocities. To solve the latter problem, we use the time-discrete variational geodesic calculus of [25] as described in [6].

The Karcher mean $\bar{c}$ of a set $\{c_1, \ldots, c_n\}$ of curves is defined as the minimizer of

$$F(c) = \frac{1}{n} \sum_{j=1}^{n} \mathrm{dist}(c, c_j)^2. \tag{4}$$

It can be computed by iteratively solving initial and boundary value problems for geodesics. We refer to [23] for more details.

4 Numerical examples

4.1 Data acquisition and setup

We tested our implementation on a dataset of shapes collected by the Computer Vision Group at Brown university [14]. The dataset consists of black and white images of physical objects. It is natural to represent the objects by their boundaries using unparametrized curves. In addition to factoring out reparametrizations, we also factor out translations and rotations because we are not interested in the position of the curves in space. Some of the resulting

□

Figure 5: First column: Karcher means (bold) of the groups of fish and humans. Second and third column: geodesics from the mean in the first and second principal direction at the times $-3, -2, \ldots, 2, 3$; the bold curve is the mean.

Next, we represented each shape in the group by the initial velocity from the mean $\bar{c}$ using the inverse of the Riemannian exponential map. We then performed a principal component analysis with respect to the inner product $G_{\bar{c}}$ on the set of initial velocities. In the group of human figures, the first three eigenvalues capture 67%, 22%, and 6% of within-group variation. In the group of fish, the first three eigenvalues capture only 40%, 25%, and 16% of within-group variation. Geodesics from the mean in the directions of the first two principal directions can be seen in Fig. 5. In the group of humans the first principal direction encodes bending of the arms and legs, whereas the second direction reflects stretching in the extremities.

5 Conclusions

In this article we developed a numerical framework for solving the initial and boundary value problem for geodesics of planar, unparametrized curves under second order Sobolev metrics. We tested our implementation on a dataset of shapes representing various groups of similar physical objects and obtained good experimental results. In future work, we plan to apply our algorithms to datasets of real-world medical data, prove rigorous convergence results for the discretization, and extend the framework to other spaces of mappings like manifold-valued curves and embedded surfaces.

Acknowledgements

▭